

Scientific Paper

Doi: <http://dx.doi.org/10.1590/1809-4430-Eng.Agric.v43n6e20230054/2023>

FULL-POWERSHIFT ENERGY BEHAVIOR TRACTOR IN SOIL TILLAGE OPERATION

**Gabriel G. Zimmermann^{1*}, Samir P. Jasper¹, Daniel Savi¹,
Tiago R. Francetto², Jorge W. Cortez³**

^{1*}Corresponding author. Universidade Federal do Paraná/Curitiba - PR, Brasil.

E-mail: gabrielganancini@gmail.com | ORCID ID: <https://orcid.org/0000-0002-9709-4458>

KEYWORDS

velocity, fuel consumption, operating efficiency.

ABSTRACT

Operational speed influences the soil preparation quality, the first established according to the working set performance and its traction capacity. The experiment's objective is to determine the influence of working speed on energy and operational performance of an agricultural tractor with Full-Powershift transmission when performing a harrowing operation. We conducted the experiment using lines, in a randomized block design. It had four operational soil preparation speeds, with seven repetitions, totaling 28 experimental units. We measured the following parameters per worked area: slipping, engine rotation, specific and per hour fuel consumption, strength, power, and yield on the drawbar and operating speed. Additionally, we analyzed soil profilometry parameters concerning the mobilized area and working thickness. We also evaluated the variance of the collected data and, when significant, submitted it to a regression test. The data showed that higher operating speeds result in greater operational performance and reduction of the energy demand of the mechanized set under study. In addition, this increase doesn't have a beneficial effect on grid fluctuation, not affecting the quality of soil preparation.

INTRODUCTION

One of the decisive operations among conventional farming practices is soil preparation. It requires significant energy demand from the mechanized set, besides being responsible for a large part of production costs. However, the correct sizing of agricultural tractors provides powertrain optimization, resulting in reduced fuel consumption, working time, and emission of pollutants into the environment (Janulevičius & Damanauskas, 2023).

Among the various variables analyzed to determine a tractor's operational and energetic performance, we underline the wheel-spinning, speed and respective fuel consumption, power and yield on the drawbar, specific fuel consumption, and the engine thermal efficiency (Strapasson Neto et al., 2020; Zimmermann et al., 2022a).

According to Martins et al. (2021), the revolved soil volume and fuel consumption during soil tillage are directly related to the set operational speed. However, Pequeno et al. (2012), when analyzing the performance of light harrowing

with cutout discs, found that the speed increase reduced the grid's acting depth, creating the effect called fluctuation.

The operating speed behavior for the heavy harrowing is an unusual theme, once this equipment differs from the light harrowing in terms of number, spacing, and diameter of discs. Furthermore, another relevant feature is the total mass of the implement and its disk-to-disk distribution, which is much heavier. These factors decrease the undesirable effects of the speed increase in harrowing, avoiding harrow fluctuation (Damanauskas & Janulevičius, 2022).

Presently, different transmission types are provided by the national and international markets, especially the Full-Powershift transmission model (Strapasson Neto et al., 2022). This transmission operates by adjusting the gears and engine rotation through an electronic manager, coupling gears in an electro-hydraulic mode, with a limited number of gears (Li et al., 2019; Siddique et al., 2023).

Thus, in the current literature there is little research related to the performance of the Full Powershift transmission system with soil preparation operations,

¹ Universidade Federal do Paraná/Curitiba - PR, Brasil.

² Universidade Federal de Santa Maria/Cachoeira do Sul - RS, Brasil.

³ Universidade Federal de Grande Dourados/Dourados - MS, Brasil.

Area Editor: Murilo Mesquita Baesso

Received in: 4-3-2023

Accepted in: 10-17-2023



making it necessary to carry out studies related to this topic to determine operational and energetic behaviors, in addition to its effect on the quality of soil preparation. The objective was to determine the influence of working speed on the energetic and operational performance of an agricultural tractor with Full-Powershift transmission. It also aimed to establish this factor's effect on harrowing operation quality parameters.

MATERIAL AND METHODS

We conducted the study in the city of Pinhais (PR), Brazil (25° 23' 40" S, 49° 07' 22" W; altitude 910 m asl). The climate is classified as Cfb (humid subtropical without dry season) and receives mean annual precipitation between 1400 and 1600 mm. The soil is a clayey-textured Oxisols.

TABLE 1. Soil characterization. Soil penetration resistance (RP), soil density (DS), volumetric humidity (UV), liquid limit (LL), plastic limit (LP) and plasticity index (IP).

Depths (m)	RSP (MPa)	DS (g cm ⁻³)	UV (g g ⁻¹)	LL (g g ⁻¹)	LP (g g ⁻¹)	IP (g g ⁻¹)
0.00-0.10	0.90	1.25	30.09	37.50	29.17	8.40
0.10-0.20	2.87	1.34	30.26			
0.20-0.30	3.51	1.29	30.48			

We prepared the mobilized soil strips with the SGAC 14c heavy grid (Civemasa®). It had 14 cutout disks of 30 inches in diameter, spaced 0.36 m (totaling a working width of 2.34 m), and a total mass of 3,150 kg. We coupled the implement to the traction bar of a New Holland® tractor, model T7 260, with net potency (DIN 70020) of 160.92 kW at 2200 rpm. It had an 18 x 6 Full Powershift transmission with 495 hours of use, sized according to ASABE D496.3 (2011). During the soil preparation, the tractor operated with front-wheel assist and locked differential.

We equipped the tractor with single radial tires at the front, model 600/65R28 Pirelli® under 68.95 kPa (10 psi) of pressure, and double radial tires at the rear 520/85R24 Firestone® the two under 62.05 kPa (09 psi) of pressure. It resulted in an advance rate of 1.60%. We added 40% water to the front axle wheels and 25% to the rear axle wheels for ballasting. We used lower (450 kg) and vertical (10 plates with 45 kg each) metal ballasts in the front, and eight rings (227 kg each) at the rear, resulting in 12,300 kg of mass. Applying it this way, we distributed the mass 35% in the front axle and 65% in the rear axle (Schlosser et al., 2020), and the power mass ratio was 76.43 kg kW⁻¹.

To evaluate the specific resistance and energetic demand for soil tillage, we equipped the tractor with a data acquisition system (DAS) with a printed circuit board and wireless communication. The system acquired the data with a frequency of one hertz, transferring it to a hard disk for posterior tabulation and analysis. The DAS had the sensors described below.

We determined the drive wheels slipping using encoders Autronics® E50S8-360-3T-24, operating with and without load, calculated according to [eq. (1)].

$$WS = \left(\frac{n_1 - n_0}{n_0} \right) \times 100 \quad (1)$$

Where:

WS – wheel slipping in %;

We determined the penetration resistance of the soil (RP) with a portable electronic penetrometer, model PLG 1020 (Falker®), configured to acquire data every 0.01 m until achieving 0.3 m deep. During the evaluation of RP, we also collected soil samples in the following depths: 0.0-0.10, 0.10-0.20 e 0.20-0.30 m, to determine the density (Ds) and volumetric humidity (Vh), according to Embrapa (2017). The determination of soil consistency followed the methodology of the twenty-five shell blows on the base of Casagrande's apparatus. We used Embrapa's (2017) technique to define the plasticity limit. It corresponds to the soil consistency at the transition from the plastic state to the semi-solid state. The difference between the values indicates the soil's plasticity index, as shown in Table 1.

n_0 – number of unladen wheel pulses, and

n_1 – number of loaded wheel pulses.

We obtained the gear ratio between the crankshaft and the power take-off employing a digital tachometer Victor® model DM6236P, establishing the reduction ratio of 3.63 ($R^2 = 0.99$). We measured the engine rotation (ER) by monitoring the rotation regime of the power take-off, with an Autronics® encoder, model E50S8-360-3-T-24.

For measuring the hourly fuel consumption (HFC), we installed flowmeters model LSF 45L0-M2 Flowmate OVAL MIII®. They allocate in the fuel supply system (at the inlet before the filter after the sediment cup) and in the common return (pump, injection nozzles, and common rail). The difference in the number of pulses emitted by the flowmeters allows us to obtain the volumetric fuel consumption, with an accuracy of 0.001 liters per pulse ($R^2 = 0.99$).

We measured the force on the drawbar (FD) using a Bermann® load cell, with a capacity of 196 kN, a sensitivity of 2.0 + 0.002 Mv V⁻¹, and an accuracy of 0.01 kN ($R^2 = 0.99$). We calibrated it appropriately and installed it on the drawbar coupled to the tractor.

To obtain the operational speed (OS), we used the SVA-60 speed antenna (Agrosystem®). It allowed us to quantify the displacement as a function of emitted pulses number ($R^2 = 0.99$).

We obtained the potency available on the drawbar with a function of force and speed, according to [eq. (2)].

$$PDB = FDB \times VO \quad (2)$$

Where:

PDB – power on the drawbar, kW.

From the power available on the drawbar and tractor's engine, we could determine the yield on the drawbar according to [eq. (3)].

$$YD = \left(\frac{PDB}{EP} \right) \times 100 \quad (3)$$

Where:

YD – yield on the drawbar, %, and

EP – engine potency, kW.

We obtained the diesel density based on the temperatures acquired by type K thermocouples, installed next to the flowmeter in the return of the fuel to the tank, and adjusted with [eq. (4)].

$$D = 844,14 - (0,53 \times T) \quad (4)$$

Where:

D – Diesel oil density, g L⁻¹;

T – Diesel oil temperature, °C, and

844.14 and 0.53 – Density regression parameters.

We calculated the hourly, mass-based, fuel consumption according to [eq. (5)].

$$HCM = \left(\frac{HCV \times D}{1000} \right) \quad (5)$$

Where:

HCM – hourly fuel consumption based on mass, g h⁻¹;

HCV – hourly fuel consumption based on volume, L h⁻¹, and

1000 - Conversion factor.

We determined the specific fuel consumption considering the hourly, mass-based, consumption, due to the power on the bar, according to [eq. (6)].

$$SFC = \left(\frac{HCM}{PDB} \right) \quad (6)$$

Where:

SFC – specific fuel consumption, g kW h⁻¹.

We used a conventional profilometer, with 56 metal rods spaced every 0.05 m, to monitor the effect of speed on the heavy grid operation depth. It totalized a reading perimeter corresponding to 2.80 m. We followed the soil profilometry methodology proposed by Carvalho Filho et al. (2007).

We obtained the calculations of the elevation area and the mobilized area (AM) through the Simpson Rule (Equation 7), according to Uddin et al. (2019).

$$\int_{X_0}^{X_n} dx = \frac{h}{3} (f_0 + 4f_1 + 2f_2 + 4f_3 + 2f_4 + \dots + 2f_{n-2} + 4f_{n-1} + f_n) \quad (7)$$

Where:

$$h = \frac{X_n - X_0}{n}, X_n > X_0$$

and where,

n – number of intervals;

f – height of quotas, mm;

h – distance between quotas, cm, and

X – number of quotas.

After obtaining the mobilized soil profile data, we determined the average thickness (AT) with [eq. (8)].

$$AT = \frac{Ma}{L_p} \quad (8)$$

Where:

AT – average thickness of the mobilized layer, m;

Ma – mobilized area of soil, m², and

L_p – length of the profilometer, m.

We calculated the operational field capacity (OFC) using [eq. (9)]. We used the values of 2.34 m (WW) and 80% (OE).

$$OFC = \frac{OS \times WW \times OE}{10} \quad (9)$$

Where:

OFC – operational field capacity, ha h⁻¹;

WW – working width, m, and,

OE – operating efficiency, %.

We determined the fuel consumption per area worked according to Soranso et al. (2008), using [eq. (10)].

$$FCA = \frac{HCV}{OFC} \quad (10)$$

Where:

FCA – fuel consumption per area worked, L ha⁻¹.

We experimented in lines, with a randomized block design, consisting of four operational soil preparation speeds (5.7, 6.8, 8.2, and 9.8 km h⁻¹), obtained in gears F7, F8, F9, and F10, operating with the rotation of the tractor's engine set at 2,200 rpm. For each treatment, we performed seven repetitions in ranges of 50 meters, totaling 28 experimental units.

We submitted the collected data to normality tests (Shapiro-Wilk) and variance homogeneity (Levene). Given these assumptions, we applied variance analysis, using the statistical program Sigmaplot 12 (Systat®). When the F testing showed significance (p ≤ 0.05 of probability), we applied the polynomial regression test, selected with the greater R² criteria and significance (p ≤ 0.05) for equation parameters.

RESULTS AND DISCUSSION

Table 2 and 3 shows the synthesis and the results of the analyzed data. It shows the energy demand in the soil preparation and quality of the operation, respectively, with no need for transformation of the means, denoting normality of the variances (Shapiro-Wilk) for all parameters. Additionally, WS, ER, HCV, OS, PDB, YD, AM, AT, and FCA exhibited variance residues homogeneity (Levene). On the other hand, the coefficient of variation of the soil preparation quality parameters presented an average of 19.70%. It can be associated with the variability of the physical attributes in the experimental area, as explained by Francetto et al. (2021).

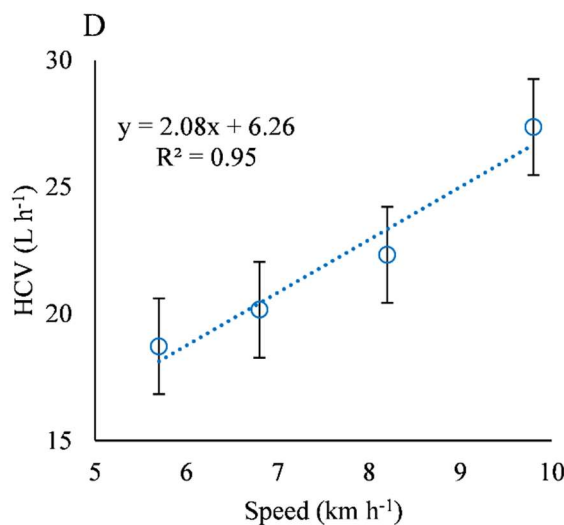
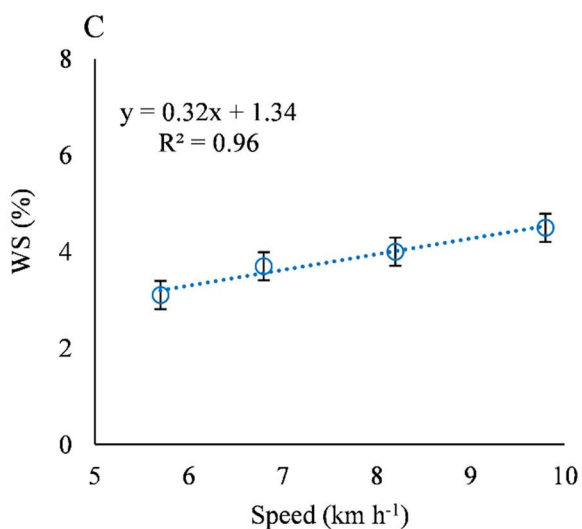
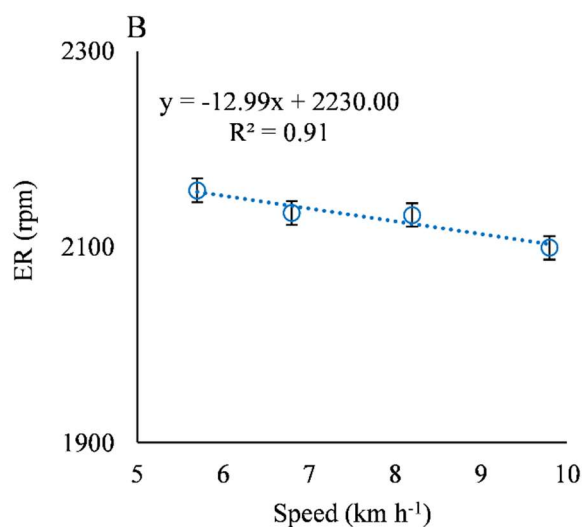
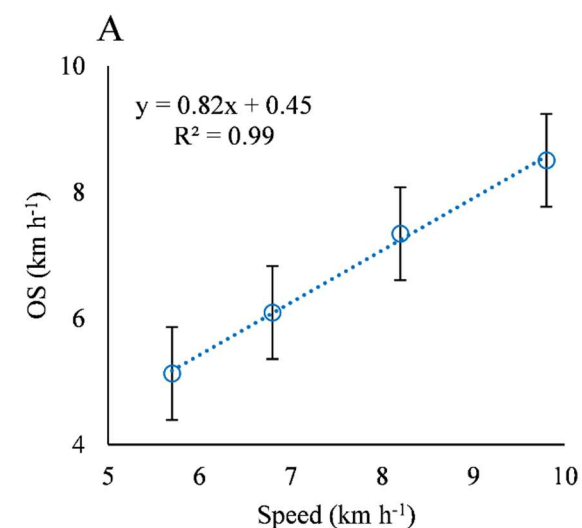
TABLE 2. Statistical synthesis of the analysis of variance for the evaluated variables.

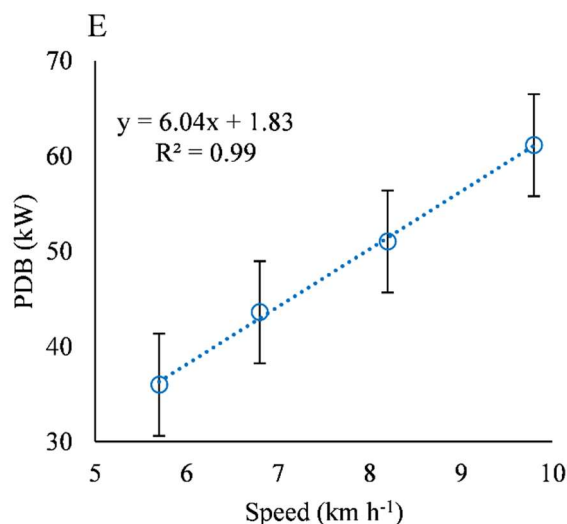
Analysis	Evaluated variables					
	WS (%)	ER (rpm)	HCV (L h ⁻¹)	FDB (kgf)	OS (km h ⁻¹)	PDB (kW)
Normality						
SW	0.069	0.138	0.062	0.191	0.070	0.190
Homogeneity						
LEV	0.414	0.120	0.125	0.027	0.432	0.260
F test	2.797*	255.862**	9.19**	0.473 ^{NS}	2657.601**	73.506**
CV (%)	9.75	0.16	12.60	4.47	0.94	5.84

Variables: Skidding (WS), Engine rotation (ER), Hourly fuel consumption (HCV), Strength on the drawbar (FDB), Operating speed (OS) and Power on the drawbar (PDB). Shapiro-Wilk Normality Test: $SW \leq 0.05$ – Data abnormality; $SW > 0.05$ – Normality in data. Levene's variance homogeneity test: $LEV \leq 0.05$ – Heterogeneous variances; $LEV > 0.05$ – Homogeneous variances. Analysis of variance (ANOVA) F-test: NS – Not significant; * ($p \leq 0.05$) and ** ($p \leq 0.01$). CV: Coefficient of Variation.

The obtained results illustrate the difference in the operational speed over WS, ER, HCV, OS and PDB. For the FDB variable, there was no distinction between the analyzed operational speeds, demonstrating the stability of the tractive force demanded during the treatments.

Analyzing the effect of speed on the variables under study (Figure 1), we observed the linear behavior for OS, ER, WS, HCV and PDB, with a determination coefficient higher than 91%.





Vertical bar - Standard error.

FIGURE 1. Regression of the velocity factor on the variables operating speed (OS), engine rotation (ER), skidding (WS), hourly fuel consumption (HCV) and power on the drawbar (PDB).

Checking the operating speed (Figure 1A), it reveals a linear increase in relation to the selected speed. According to the acquired equation, the set moved on 18% below the selected speed, a fact explained due to the Full-Powershift transmission architecture having a fixed number of relationships (Li et al., 2019; Mattetti et al., 2019). This factor, in addition to the low variation of engine rotation, corroborates with Vantsevich (2007).

We set the engine rotation at 2,200 rpm at the beginning of the experimental line, but this variable kept decreasing (Figure 1B), with the increase in the selected speed. It is an event explained by the engine's heavier load, due to the rise in traction potency.

Concerning slipping (Figure 1C), there is a linear growth at the expense of the selected speed, which according to the obtained equation, the smaller slipping rate (3.2%) occurred at the speed of 5.7 km h⁻¹. It can be explained by the

slipping index rising with the increase in power demand at higher operating speeds (Monteiro et al., 2011; Kmiecik et al., 2023). These values were lower than those established by ASABE D496.3 (2011) for firm soils, which according to Gabriel Filho et al. (2010), also applies to covered surfaces. In those, the values vary between 8 and 10% due to the size of the operational set remaining overestimated.

For HCV (Figure 1D), coherent values (Jasper et al., 2016) are first observed around the desired speeds, resulting in an increase of 2.1 L h⁻¹ by one kilometer per hour. This phenomenon explains itself with the increment of power in the drawbar (Figure 1E), associated with the decrease in engine speed, causing the fuel supply system to inject more into the engine, making it work with greater consumption. Martins et al. (2018) observed a similar fact when monitoring the HCV in the intermediate harrowing in clayey soils.

TABLE 3. Statistical synthesis of the analysis of variance for the evaluated variables.

Analysis	Evaluated variables				
	YD (%)	SFC (g kW h ⁻¹)	AM (m ²)	AT (m)	FCA (L ha ⁻¹)
Normality					
SW	0.148	0.789	0.594	0.647	0.095
Homogeneity					
LEV	0.270	0.043	0.065	0.072	0.421
F test	73.505**	3.786**	0.159 ^{NS}	0.197 ^{NS}	2.067 ^{NS}
CV (%)	5.85	9.12	19.31	20.03	12.02

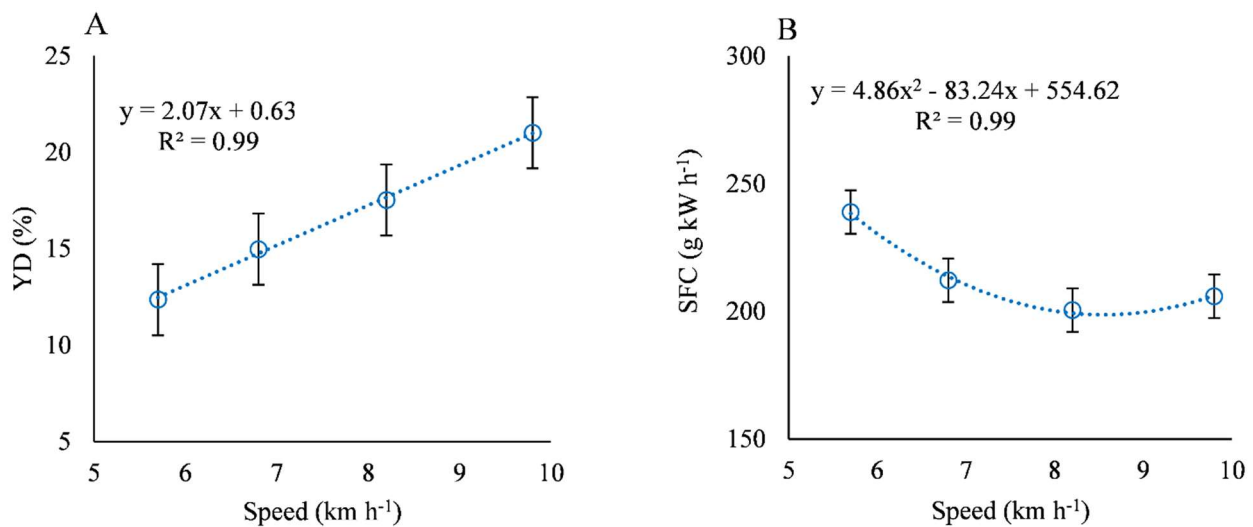
Variables: Yield on the drawbar (YD), Specific fuel consumption (SFC), Mobilized area (AM), Average thickness (AT) and Fuel consumption per worked area (FCA). Shapiro-Wilk Normality Test: SW ≤ 0.05 – Data abnormality; SW > 0.05 – Normality in data. Levene's variance homogeneity test: LEV ≤ 0.05 – Heterogeneous variances; LEV > 0.05 – Homogeneous variances. Analysis of variance (ANOVA) F-test: NS – Not significant; * (p ≤ 0.05) and ** (p ≤ 0.01). CV: Coefficient of Variation.

There was difference in operational speed on YD and SFC. For the FCA variable, there was no distinction between the analyzed operational speeds, as explained for variable FDB. For the mobilized area and average thickness, the quality parameters are stable during soil preparation, with no significant variation in these factors due to the

increase in the operational speed. This effect may be associated with friable soil consistency at the experimenting time, as described by Francetto et al. (2016).

Considering AT and AM, the means didn't show significance. Soil preparation equipment is influenced by the operating speed, which affects the working depth of the

machinery, which is called fluctuation. However, in the study in question, there was no significant interference from speed, making it impossible to observe this phenomenon, which is explained by the high mass of the implement used (Martins et al., 2021).



Vertical bar - Standard error.

FIGURE 2. Regression of the velocity factor on the variables yield on the drawbar (YD) and specific fuel consumption (SFC).

Analyzing the effect of speed on YD (Figure 2A) an increase of 2.07% is observed with the increase of 1 km h⁻¹, added to the 0.63% resulting from displacement speed and the relation between tractor weight and power. This can be explained by the fact that this parameter varies depending on the magnitude of the torque that the engine-transmission set is capable of applying to the drive wheels, according Strapasson Neto et al. (2022).

The SFC (Figure 2B) demonstrates the quadratic-polynomial behavior of the speeds operated by the set. The lower speed demanded more energy per produced potency, though using the remaining ones consumed less energy and did not differ within themselves. For the determined equation, the lowest SFC (198 g kW h⁻¹) occurs by harrowing at a speed of 8.56 km h⁻¹. The result fits the premise reported by Farias et al. (2017), that the set must exhibit SFC values below 200.0 g kW h⁻¹ to be considered efficient.

According to the prior presented results, it is possible to verify the maintenance of harrowing quality with the escalation of the speed, which allows the achievement of higher energy levels and operational performance of the mechanized set. Therefore, the transformation of the mechanical energy produced by the engine is maximized and provides the most efficient use of fossil fuels in contemporary agriculture (Balsari et al., 2021; Zimmermann et al., 2022 b).

Higher operational and energetic efficiency rates when using higher speeds without impairing the soil tillage emphasize the possibility of working at higher speeds than those recommended by Martins et al. (2018).

CONCLUSIONS

Increasing the operating speed resulted in higher efficiency and reduced energy demand of the mechanized set. That is due to the Full-Powershift transmission system acting appropriately over the studied variables.

In Figure 2, we observe the linear behavior for YD, with a determination coefficient greater than 99%. We also determined a second-order polynomial for SFC, with a coefficient of determination greater than 99%.

The increase in the operating speed of the tractor-grid set does not increment grid fluctuation nor diminish the soil preparation quality, due to the weight of the equipment.

REFERENCES

- ASABE - American Society of Agricultural Biological Engineers (2011) ASABE 496.3 Agricultural machinery management data. In: ASABE Standards: standards engineering practices data. St. Joseph, 372p.
- Balsari P, Biglia A, Comba L, Sacco D, Alcatrao LE, Varani M, Aimonino DR (2021) Performance analysis of a tractor-power harrow system under different working conditions. *Biosystems Engineering* 202:28-41. <https://doi.org/10.1016/j.biosystemseng.2020.11.009>
- Carvalho Filho A, Centurion JF, Silva RPD, Furlani CE, Carvalho LC (2007) Soil tillage methods: alterations in the roughness of the soil. *Engenharia Agrícola* 27(1):229-237. <https://doi.org/10.1590/S0100-69162007000100017>
- Damanauskas V, Janulevičius A (2022) Effect of tillage implement (spring tine cultivator, disc harrow), soil texture, forward speed, and tillage depth on fuel consumption and tillage quality. *Journal of Agricultural Engineering* 53(3):1-10. <https://doi.org/10.4081/jae.2022.1371>
- EMBRAPA - Empresa Brasileira de Pesquisa Agropecuária (2017) Serviço Nacional de Pesquisa de Solos: Manual de Métodos de Análise de Solo. Brasília, 577p.
- Farias MSD, Schlosser JF, Martini AT, Santos GOD, Estrada JS (2017) Air and fuel supercharge in the performance of a diesel cycle engine. *Ciência Rural* 47(6):1-7. <http://dx.doi.org/10.1590/0103-8478cr20161117>

- Francetto TR, Alonço ADS, Becker RS, Scherer VP, Bellé MP (2021) Effect of the Distance between the Cutting Disc and Furrow Openers Employed in Row Crop Planting on Soil Mobilization. *Engenharia Agrícola* 41(2):148-160. <https://doi.org/10.1590/1809-4430-Eng.Agric.v41n2p148-160/2021>
- Francetto TR, Alonço ADS, Brandelero C, Machado ODDC, Veit AA, Carpes DP (2016) Disturbance of Ultisol soil based on interactions between furrow openers and coulters for the no-tillage system. *Spanish Journal of Agricultural Research* 14(3):1-10. <https://doi.org/10.5424/sjar/2016143-9148>
- Gabriel Filho A, Lanças KP, Leite F, Acosta JJ, Jesuino PR (2010) Desempenho de trator agrícola em três superfícies de solo e quatro velocidades de deslocamento. *Revista Brasileira de Engenharia Agrícola e Ambiental* 14:333-339.
- Janulevičius A, Damanauskas V (2023) Validation of relationships between tractor performance indicators, engine control unit data and field dimensions during tillage. *Mechanical Systems and Signal Processing* 191:110201. <https://doi.org/10.1016/j.ymsp.2023.110201>
- Jasper SP, Bueno LDSR, Laskoski M, Langhinotti CW, Parize GL (2016) Desempenho do trator de 157KW na condição manual e automático de gerenciamento de marchas. *Scientia Agraria* 17(3):55-60.
- Kmiecik LL, Jasper SP, Passos ML, Strapasson Neto L, Zimmermann GG, Savi D, Parize GL (2023) Agricultural tractor with different mass distributions between axles. *Ciência Rural* 53(3):1-9. <http://doi.org/10.1590/0103-8478cr20210604>
- Li B, Sun D, Hu M, Zhou X, Liu J, Wang D (2019) Coordinated control of gear shifting process with multiple clutches for power-shift transmission. *Mechanism and Machine Theory* 140:274-291. <https://doi.org/10.1016/j.mechmachtheory.2019.06.009>
- Martins MB, de Almeida Prado Bortolheiro FP, Testa JVP, Sartori MMP, Crusciol CAC, Lanças KP (2021) Fuel consumption between two soil tillage systems for planting sugarcane. *Sugar Tech* 23(1):219-224. <https://doi.org/10.1007/s12355-020-00873-4>
- Martins MB, Sandi J, de Souza FL, de Souza Santos R, Lanças KP (2018) Otimização energética de um trator agrícola utilizando normas técnicas em operações de gradagem. *Revista Engenharia na Agricultura* 26(1):52-57. <https://doi.org/10.13083/reveng.v26i1.852>
- Mattetti M, Maraldi M, Sedoni E, Molari G (2019) Optimal criteria for durability test of stepped transmissions of agricultural tractors. *Biosystems Engineering* 178:145-155. <https://doi.org/10.1016/j.biosystemseng.2018.11.014>
- Monteiro LDA, Lanças KP, Guerra SP (2011) Performance of an agricultural tractor equipped with radial and bias ply tires on three levels of liquid ballast. *Engenharia Agrícola* 31(3):551-560. <https://doi.org/10.1590/S0100-69162011000300015>
- Pequeno ID, Arcoverde SNS, Cortez JW, Garrido MS, Carvalho PGS (2012) Desempenho operacional de conjunto trator-grade em argissolo amarelo no semiárido nordestino. *Nucleus* 9(2):1-10. <https://doi.org/10.3738/1982.2278.720>
- Schlosser JF, Catalán H, Bertinatto R, Farias MSD, Mas GD, Cella MC (2020) Power hop in agricultural tractors. *Ciência Rural* 50(8): 1-4. <http://dx.doi.org/10.1590/0103-8478cr20200199>
- Siddique MAA, Baek SM, Baek SY, Jeon HH, Kim YJ, Kim YS, Kim TJ (2023) Application of auto power shift (APS) controller for minimizing fuel consumption and performance evaluation of an agricultural tractor. *Computers and Electronics in Agriculture* 214(1):108279. <https://doi.org/10.1016/j.compag.2023.108279>
- Soranso AM, Gabriel Filho A, Lopes A, Souza EGD, Dabdoub MJ, Furlani CE, Camara FTD (2008) Desempenho dinâmico de um trator agrícola utilizando biodiesel destilado de óleo residual. *Revista Brasileira de Engenharia Agrícola e Ambiental* 12(5):553-559.
- Strapasson Neto L, Kmiecik LL, Jasper SP, Zimmermann GG, Savi D (2020) Interference of the number of remote control valves in use on the energy performance of an agricultural tractor with productivity management. *Engenharia Agrícola* 40(3):356-362. <http://dx.doi.org/10.1590/1809-4430-Eng.Agric.v40n3p356-362/2020>
- Strapasson Neto L, Zimmermann GG, Jasper SP, Savi D, Sobenko LR (2022) Energy efficiency of agricultural tractors equipped with continuously variable and full powershift transmission systems. *Engenharia Agrícola* 42(1):1-11. <http://dx.doi.org/10.1590/1809-4430-Eng.Agric.v42n1e20210052/2022>
- Uddin MJ, Moheuddin MM, Kowsher M (2019) A new study of Trapezoidal, Simpson's 1/3 and Simpson's 3/8 Rules of Numerical Integral Problems. *Applied Mathematics and Sciences: An International Journal* 6(4):1-14. <https://doi.org/10.5121/mathsj.2019.7401>
- Vantsevich VV (2007) Multi-wheel drive vehicle energy/fuel efficiency and traction performance: Objective function analysis. *Journal of Terramechanics* 44(3):239-253. <https://doi.org/10.1016/j.jterra.2007.03.003>
- Zimmermann GG, Savi D, Auler AC, Strapasson Neto L, Jasper SP (2022b) Effect of hydraulic and solid ballast on agricultural tractor performance. *Revista Ciência Agronômica* 53:1-13. <http://dx.doi.org/10.5935/1806-6690.20220059>
- Zimmermann GG, Savi D, Jasper SP, Kmiecik LL, Strapasson Neto L, Sobenko LR (2022a) Energy performance of farm tractor with single radial versus dual diagonal wheels in harrowing operations. *Revista Brasileira de Engenharia Agrícola e Ambiental* 26(5):356-364. <http://dx.doi.org/10.1590/1807-1929/agriambi.v26n5p356-364>